We are IntechOpen,
the world's leading publisher of
Open Access books
Built by scientists, for scientists

4,800
Open access books available

122,000
International authors and editors

135M
Downloads

Our authors are among the

154
Countries delivered to

TOP 1%
most cited scientists

12.2%
Contributors from top 500 universities

BOOK CITATION INDEX
CLARIVATE ANALYTICS
INDEXED

WEB OF SCIENCE™

Selection of our books indexed in the Book Citation Index
in Web of Science™ Core Collection (BKCI)

Interested in publishing with us?
Contact book.department@intechopen.com

Numbers displayed above are based on latest data collected.
For more information visit www.intechopen.com

Shear Wave Velocity Models Beneath Antarctic Margins Inverted by Genetic Algorithm for Teleseismic Receiver Functions

Masaki Kanao[1] and Takuo Shibutani[2]
*[1]National Institute of Polar Research,
Research Organization of Information and Systems, Tokyo,
[2]Disaster Prevention Research Institute,
Kyoto University, Gokasho, Kyoto,
Japan*

1. Introduction

Study on shear velocity structure of the crust and the uppermost mantle around Antarctic continent was started in the 1960's by using surface waves of the earthquakes occurred around Antarctic plate (Evison et al., 1960; Kovach and Press, 1961). Permanent seismic stations have been operated from the end of 1980's at Antarctic margins except for the South Pole (SPA) on the continental ice sheet. A majority of the stations were established as the Federation of Digital Seismographic Networks (FDSN; Butler and Anderson, 2008). The FDSN was composed of several national and governmental organizations such as the Global Seismographic Network (GSN) organized by the Incorporated Research Institutions for Seismology (IRIS), the Australian Government (AG), GEOSCOPE by French, Geo Forschungs Netz (GEOFON) by Germany, MEDNET by Italy, PACIFIC21 (Tsuboi, 1995) by Japan, and others.

In recent few years, surface wave tomography studies around Antarctic continent and surrounding oceans have been conducted by using the FDSN data (Roult et al., 1994; Ritzwoller et al., 2001; Danesi and Morelli, 2001; Kobayashi and Zhao, 2004). Enderby Land, particularly around the Napier Mountains, was one of the oldest Archaean cratons with a spatial extent about 500 km (Ellis, 1987; Black et al., 1987). However, surface wave analyses could not provide enough spatial resolution for detail discussion about fine crustal structure. Therefore, it is necessary to achieve smaller-scale heterogeneities in the specified area by using recently available broadband waveform data.

In this chapter, precise shear velocity models of the crust and the uppermost mantle were investigated from teleseismic receiver functions beneath several FDSN stations in Antarctica (Fig. 1; MAW; 67.6°S, 62.9°E, SYO; 69.0°S, 39.6°E, DRV; 66.7°S, 140.0°E, VNDA; 77.5°S, 161.9°E, PMSA; 64.8°S, 64.0°W). The obtained velocity models were discussed in relationship with the regional tectonics and crustal evolution of each terrain around the stations.
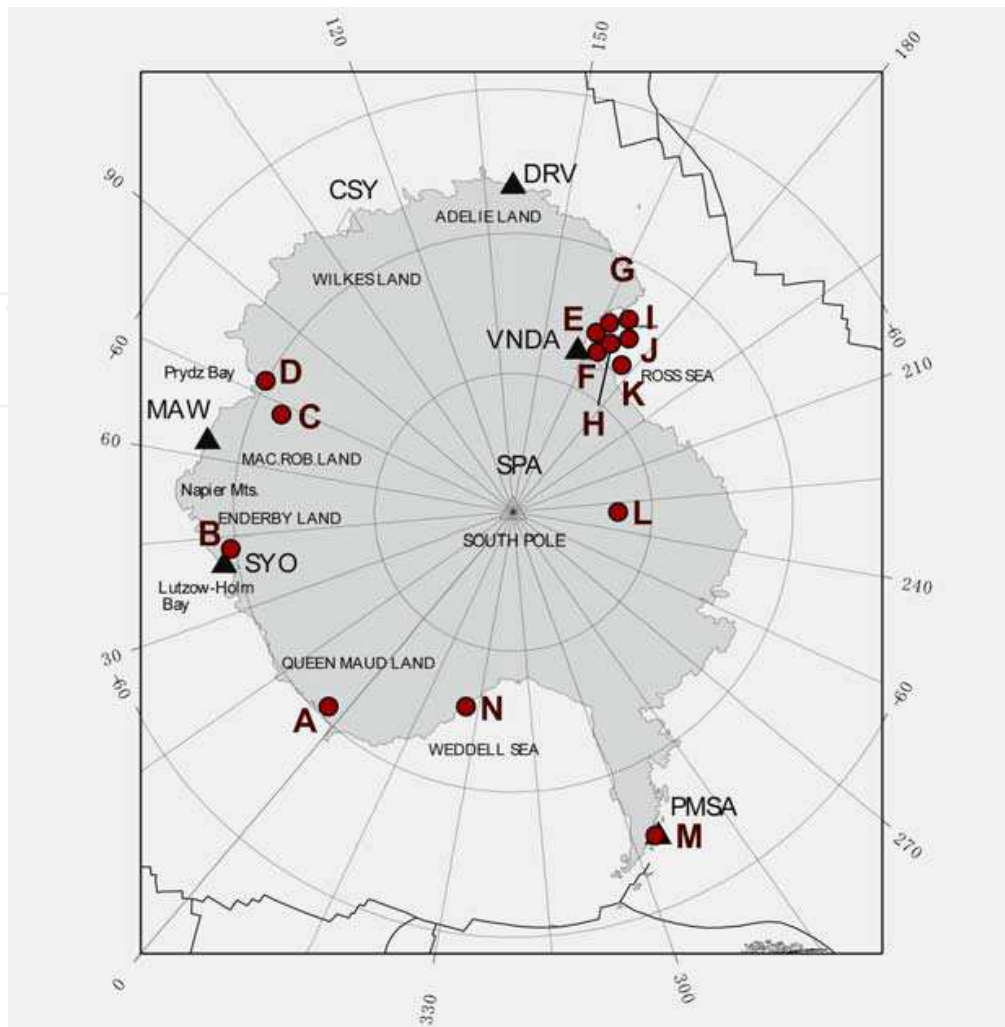
Fig. 1. Map showing the location of analyzed seismic stations by GA inversion (Solid triangles; SYO, MAW, DRV, PMSA and VNDA) in Antarctic continental margin and the related regional localities. Open triangle stations (CSY, SPA and SBA) are planned to be analyzed in future. Solid red circles are stations raveled in Von Frese et al. (1999). Alphabet numerals are location in Antarctica raveled after Von Frese et al., (1999), the same representation as in Fig. 8

2. Methodology and data

The coda parts of teleseismic P-waves contain a significant amount of information on the seismic structure in the vicinity of the recorded stations. The "receiver functions" were defined as the structural response and consisted of *P*-to-*S* converted waves and their reverberations, and were most sensitive to the shear velocity beneath the station (Fig. 2). To derive the structural response (receiver functions) beneath the recording station, the source-equalization method (Langston, 1979) was generally applied for the coda part of teleseismic P-waves. The structural response could be isolated from that of the instrument and effective source function. The followings are the procedure to produce the receiver functions.

Three components (*V, R, T*) of the total response at a station on a teleseismic *P* wave are expressed as,

$$D_V(t) = I(t) * S(t) * E_V(t)$$
$$D_R(t) = I(t) * S(t) * E_R(t) \qquad (1)$$
$$D_T(t) = I(t) * S(t) * E_T(t)$$

where $I(t)$ is the impulse response of the recording system, $S(t)$ is the effective seismic source function, and $E(t)$ implies the impulse response of the earth's structure.

For a steeply incident P wave, source equalization method (Langston, 1979) assumes,
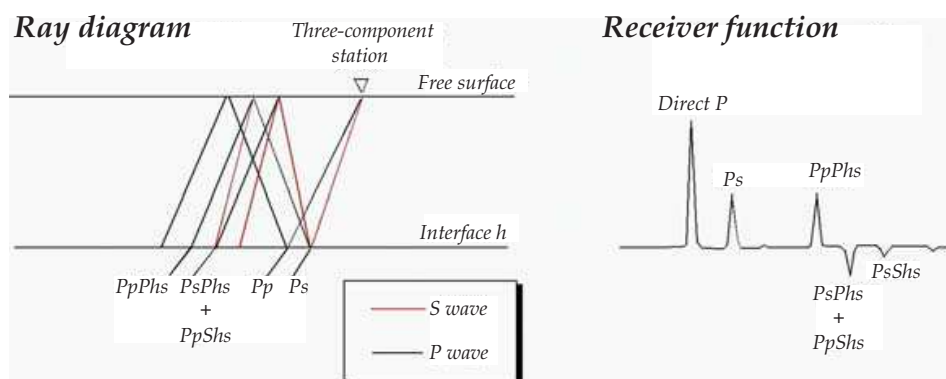
$$E_V(t) = \delta(t) \qquad (2)$$

where $\delta(t)$ is the Dirac delta function. From (1) and (2),

$$D_V(t) = I(t) * S(t) \qquad (3)$$

Thus the observed structual response $E_R(t)$ and $E_T(t)$ are available by deconvolving $D_V(t)$ from $D_R(t)$ and $D_T(t)$.

What are the receiver functions?

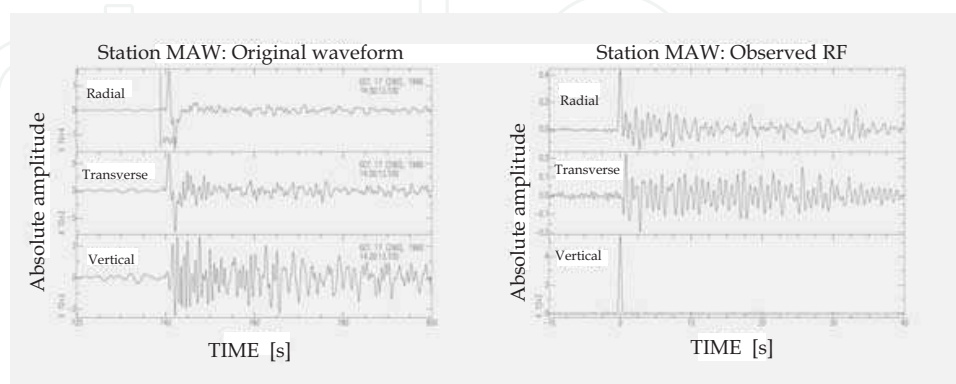

Creating receiver functions

Fig. 2. (upper) The receiver functions (RF, the crustal response) are consist of P-to-S converted waves and their reverberations, which are most sensitive to the shear velocity beneath the station. (lower) the observed receiver functions $(E_R(t)$ and $E_T(t))$ can be obtained by deconvolving the original waveforms $D_V(t)$ from $D_R(t)$ and $D_T(t)$

Since the receiver functions are sensitive to *P*-to-*S* conversions through the interfaces beneath the recording station, the waveform inversion result could produce a shear velocity structure (Owens et al., 1984; Kind et al., 1995). By applying these conventional procedures, receiver functions were obtained at five permanent FDSN stations in Antarctica.

Here, we introduce the actual procedure to create receiver functions as an example for the station MAW. Before the inversion, we used the stacked receiver functions for all 20 radial components in the backazimuth group within 70°. The incoherent noise could be suppressed by stacking the waveforms, while the coherent signals were enhanced. Dataset of teleseismic waveforms for the other four stations were the same as used in the linearlized inversion analyses by Kanao et al. (2002).

Inversion of the receiver functions to recover crustal and uppermost mantle structure have been widely recognized as sensitive to the starting model if a conventional linearization scheme was employed (Ammon et al., 1990). Prior to this study, a linearized time domain inversion was applied to determine the velocity model for several Antarctic stations (Kanao, 1997; Kanao et al., 2002). The starting model dependency might be excluded by employing a non-linear inversion scheme based on a Genetic Algorithm (GA; Sambridge and Drijkoningen, 1992; Shibutani et al., 1996).
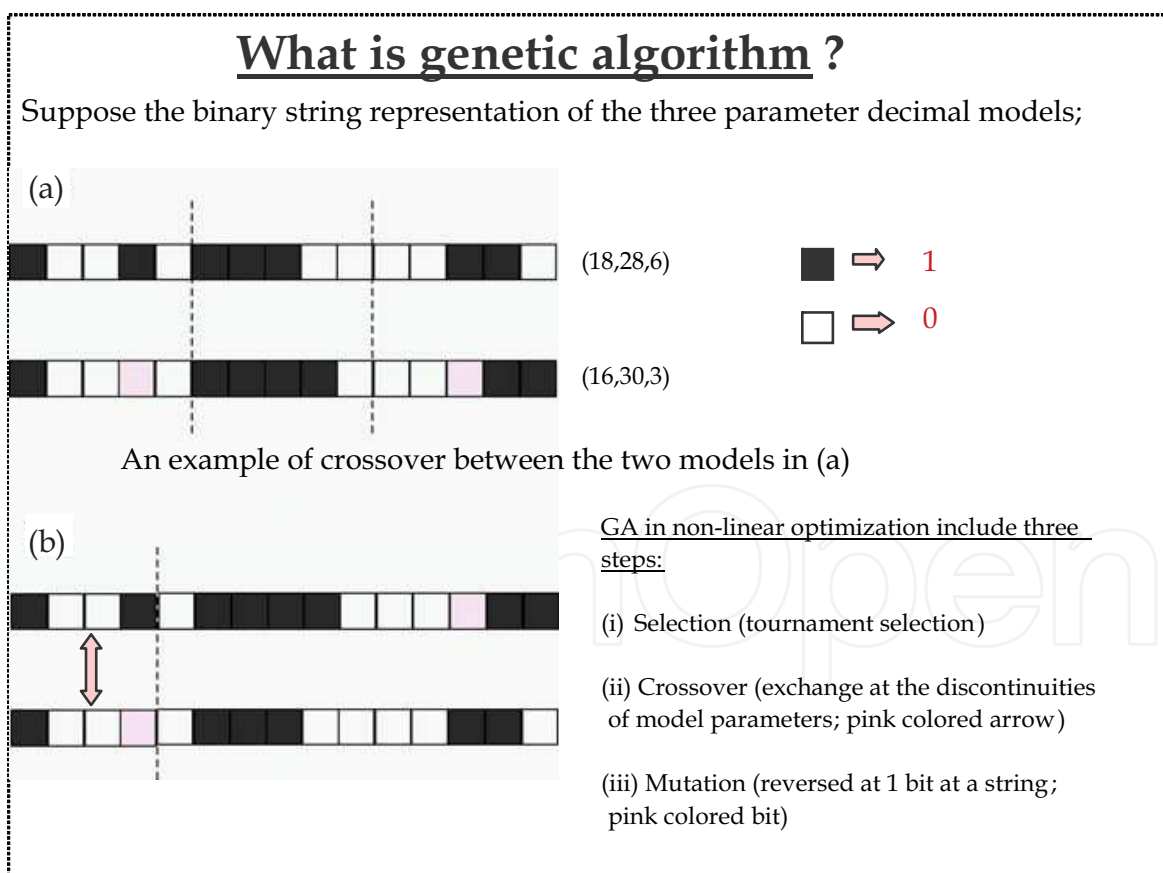

Fig. 3. Schematic illustration for Genetic Algorithm (GA). GA in non-linear optimization include three steps; (i) Selection (tounament selection), (ii) Crossover (exchange at the discontinuities of model parameters) and (iii) Mutation (reversed at 1 bit at a string), respectively. (modified after Sambridge and Drijkoningen (1992))

The GA approach makes use of a 'cloud' or 'population' of the models to minimize the dependence on a starting model; a set of 'biological' analogues are used to produce new generations of the models from previous generations, with preferential development of the models with a good fit between observed and theoretical receiver functions. Figure 3 shows a schematic illustration for GA. GA in non-linear optimization included three steps; (i) Selection (tounament selection), (ii) Crossover (exchange at the discontinuities of model parameters) and (iii) Mutation (reversed at 1 bit at a string), respectively.
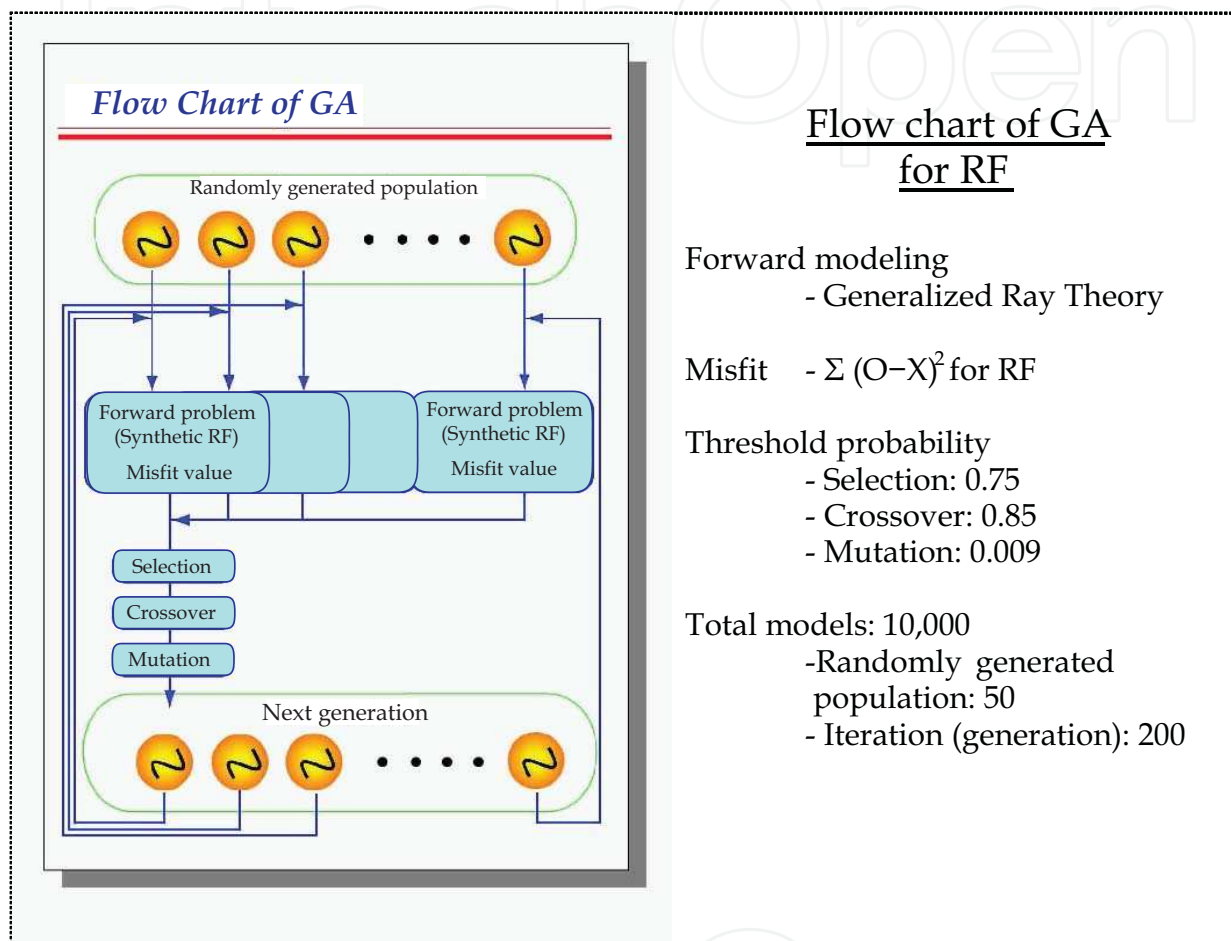

Fig. 4. Flow chart of Genetic Algorithm (GA) for receiver function inversion. Beginning with a randomly generated initial population and corresponding misfit values which are defined by square sum of the difference between the receiver function predicted for each model and that obtained from observed waveforms, succeeding populations are created by selection, crossover and mutation

In this study, a non-linear GA was applied for the stacked radial receiver functions of each station. Figure 4 represented a flow chart of GA for receiver function inversion. Beginning with a randomly generated initial population and corresponding misfit values, which were defined by the square sum of the difference between the receiver function predicted for each model and that obtained from observed waveforms, succeeding populations were created by selection, crossover and mutation procedures.

The approach provided a good sampling of the model space, and enabled the estimation of the shear-wave speed distribution within the crust, along with an indication of the ratio

between Vp and Vs. Many models with an acceptable fit to the data were generated during the inversion, and a stable crustal model was produced by employing a weighted average of the best 1,000 models encountered in the development of GA. The weighting criterion was based on the inverse of the misfit for each model, so that the best-fitting model could have the greatest influence.

For the inversion, the crust and the uppermost mantle down to 60 km were assumed to be composed from five major layers (Table 1). The model parameters in each layer were the thickness, Vs at the upper and the lower boundaries, in addition to the Vp/Vs ratio. The Vs for each layer was constructed by linearly connecting the values at the upper and the lower boundaries, so as to give a sequence of constant velocity-gradient segments separated by velocity discontinuities. The thickness and the upper and the lower limit in each layer were defined after the averaged continental crust. 'Q_α' and 'Q_β' values were assumed to be fixed in each layer on the basis of Coda-Q inversion results after Kanao and Akamatsu (1995). A smoothness constraint in the inversion was implemented by minimizing a roughness norm of the velocity model (Ammon et al., 1990).

		Basement	Crust			Mantle
			upper	middle	lower	
Thickness	lower	0.0	5.0	5.0	5.0	5.0
(km)	upper	5.0	20.0	20.0	20.0	20.0
Vs (upper)	lower	2.90	3.10	3.40	3.70	4.00
(km/s)	upper	3.90	4.10	4.40	4.70	5.00
Vs (lower)	lower	2.90	3.10	3.40	3.70	4.00
(km/s)	upper	3.90	4.10	4.40	4.70	5.00
Vp/Vs	lower	1.65	1.65	1.65	1.65	1.70
	upper	2.00	1.80	1.80	1.80	1.90
Q_α		200	300	500	800	1360
Q_β		80	120	200	300	600

Table 1. Model parameters in GA receiver function inversion. 'Vs (upper)' and 'Vs (lower)' are the S wave velocity at the upper and the lower boundaries of each layer. The 'Lower' and the 'upper' for four variables indicate the lower and the upper bounds. The thickness and the upper and the lower limit in each layer were defined after the averaged continental crust. 'Q_α' and 'Q_β' were assumed to be fixed in each layer by referring from Coda-Q inversion results after Kanao and Akamatsu (1995)

After examining the trade-off curves between the model roughness and waveform-fit residuals, we selected the most suitable pair of the above parameters. A number of iterations up to 200 times were conducted in the inversion in order to reduce the waveform-fit residuals (misfit-values) to an acceptable value, and the most stable solutions were adopted as the final models (Fig. 5). We obtained 50 population models for the every iteration. In total, we selected 10,000 models to determine the best fitted.

The waveform fits between synthetic and observed receiver functions were generally adopted, implying the adequate inversion procedures with reasonable smoothness constrained. Figure 6 represented the synthetic radial receiver functions by assuming the
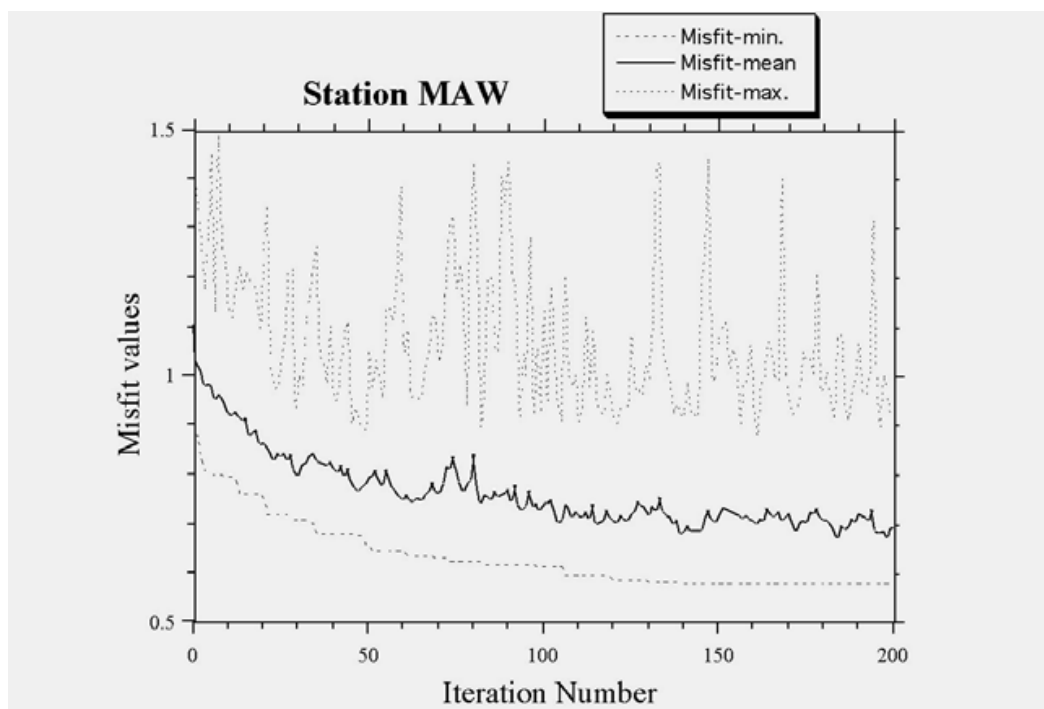
Fig. 5. Misfit values vs. the number of iteration during the GA inversion for an example of MAW. Variations in the mean, the minimum and the maximum misfit values for each population are drawn to be reached into the stable values
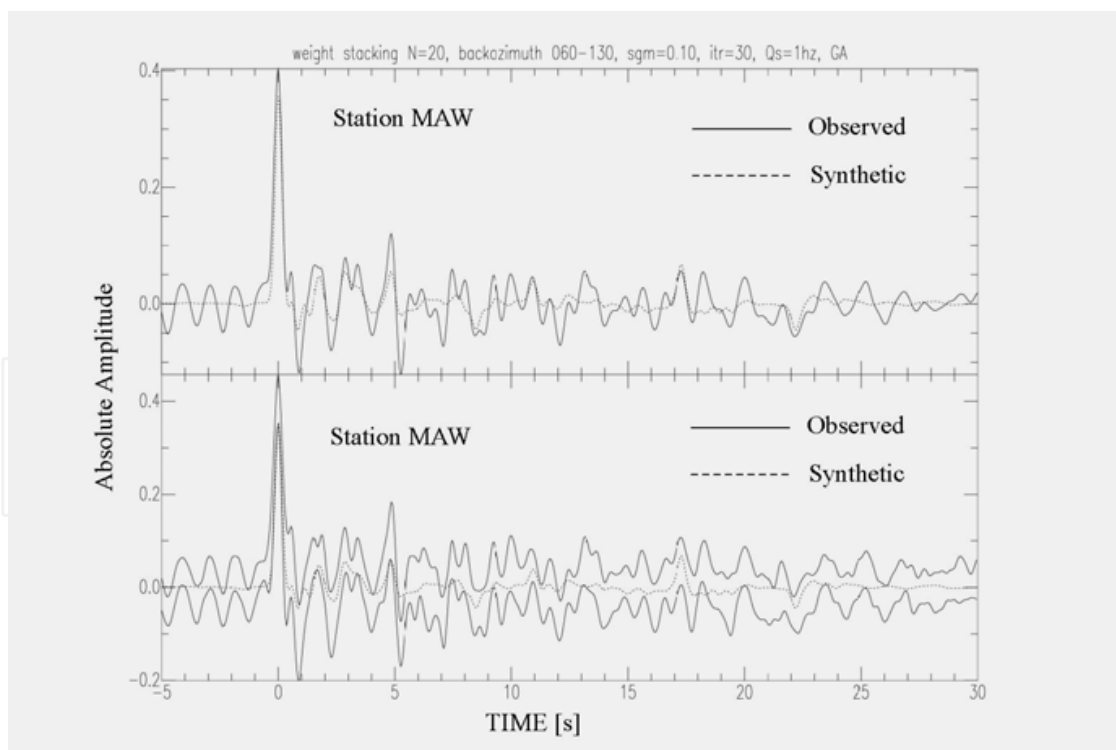

Fig. 6. Synthetic radial receiver functions by assuming the S-wave models and the Vp/Vs ratio determined by the averaged one for the best 1,000 models in the GA inversion (broken traces) compared with the observed mean (upper solid trace) and +/-1 standard error bounding (lower two solid traces) of the stacked receiver functions at MAW

S-wave models and the Vp/Vs ratio determined by the averaged one for the best 1,000 models in GA inversion (broken traces), compared with the observed mean (upper solid trace) and +/-1 standard error bounding (lower two solid traces) of the stacked receiver functions.

There were several noticeable later phases for all traces after the *P*-arrival. For example, large amplitudes were identified around 4-5 s, which were considered to be the directly converted *Ps* at the Moho discontinuity. Intra-crustal converted phases were identified around 1-2 s and 2.5-3.5 s, implying the mid-crustal velocity discontinuities. Later phases, after around 7 s, had a rather worse waveform fitting compared with the earlier phases, because of relatively poor signal-to-noise ratios for these later phases.

3. Results and discussion

In this section, we discussed the resultant shear velocity models for the individual FDSN station. Here, the averaged Vs models for the best 1000 misfits in GA inversion were mainly discussed (red lines in Figs. 7a, 7b and 7c).
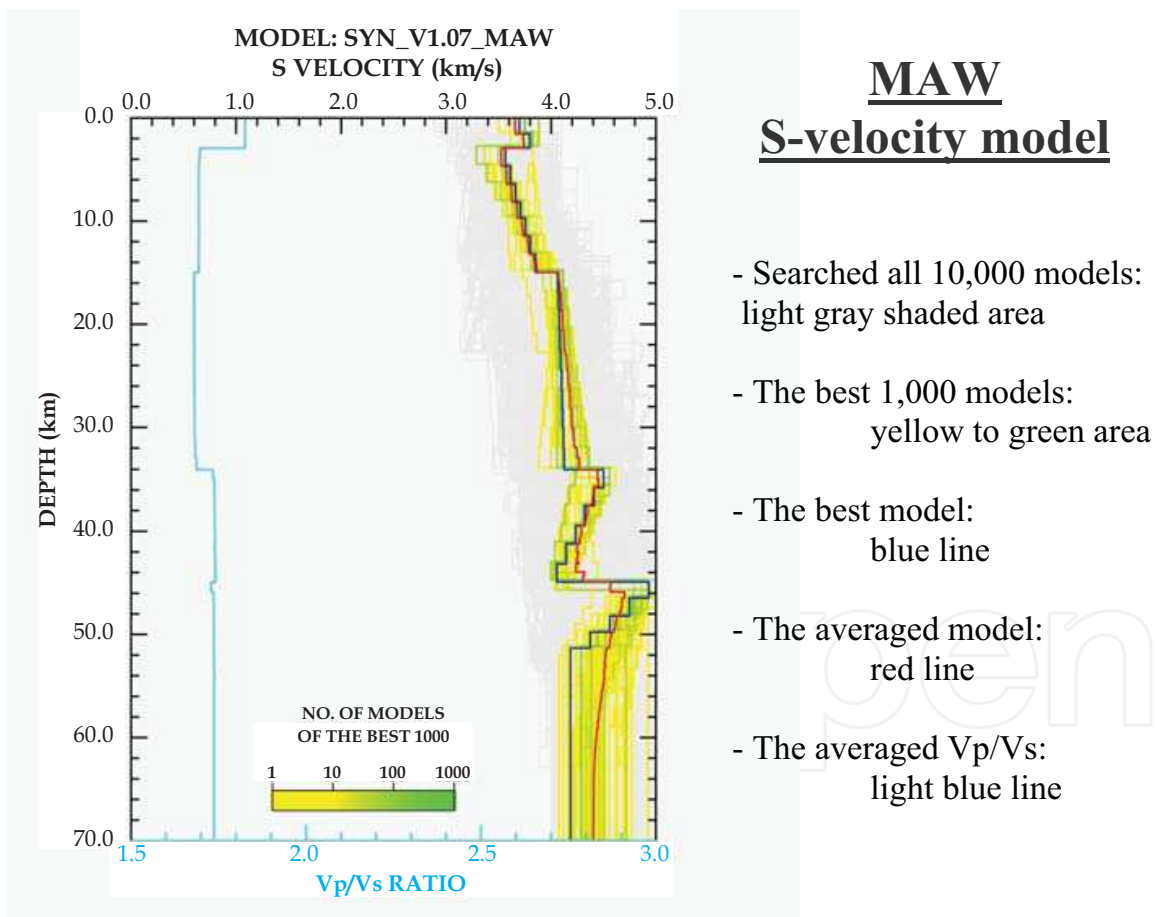

Fig. 7a. Seismic S-velocity models for MAW by GA inversion. For the S-wave velocity, all 10,000 models searched in GA inversion are shown as the light gray shaded area. The best 1,000 models are represented by the yellow to green area. The best model and the averaged model for the best 1,000 are shown by the blue line and the red line, respectively. For the Vp/Vs ratio, the light blue solid line corresponds to the averaged model

The inverted velocity model beneath MAW had a very sharp Moho discontinuity at a depth of 44 km (Fig. 7a). A discontinuity between the middle and the lower crust were recognized at 34 km depth. In Mac. Robertson Land, where MAW is located (Fig. 1), late-Proterozoic metamorphic events generated the granulite facies rocks in upper part of the crust (Tingey, 1982; Sheraton et al., 1987). The sharp and fairly deeper Moho around 44 km depth might have a relationship with the metamorphism of the Rayner Complex besides the Archaean Napier Complex. The intrusion of charnockites around MAW was an evidence of the compression tectonic setting in the Proterozoic mobile belt (Young and Ellis, 1991). Depletions of heavy rare-earth elements in the low-Ti charnockites suggested that garnet was a residual phase in partial melting, which required high pressures and an over-thickened crust. The deeper crustal thickness obtained from GA inversion at MAW appeared to be correspond with a signature of the crustal root what now have been remained as the deepened architecture comparing with the adjacent areas in Enderby Land.

The resultant velocity model around DRV (Fig. 7b, left) indicated a fairly sharp Moho at depths of 28 km. A high-velocity zone appeared in the upper and the lower crustal depths. A relatively lower velocity zone was obtained at depths around 20 km, which lied between the above two high-velocity zones. The velocities of the topmost mantle had lower values of about 4.2 km/s. In Adelie Land, where DRV is belonging (Fig. 1), a metamorphic event occurred in early-Proterozoic age (Bellair and Delbos, 1962). A rather sharp Moho and fluctuations of the crustal velocities might had been developed during the metamorphic event of the Adelie Land. In addition, high velocity zones in the upper crust together with a low-velocity discontinuity in the middle crust might be related to the early-Proterozoic tectonothermal activities.

A sharp Moho discontinuity was determined approximately at 40 km beneath SYO (Fig. 7b, right), in the Lüzow-Holm Bay region. The Moho depth was consistent with that obtained from previous large scale deep refraction / wide-angle reflection surveys around the region (Ikami and Ito, 1986; Yoshii et al., 2004). Velocity jumps were identified at 12 km and 20 km depths, which corresponded to the discontinuities between the upper-middle crust and middle-lower crust, respectively. The latter discontinuity between the middle and the lower crust significantly coincided with the depths by the recent refraction / wide-angle reflection study around the SYO (Miyamachi et al., 2003). High velocity zones in the upper crust were presumably corresponding to the granulite facies metamorphic rocks appeared in surface geology. The obtained velocities in the upper part of the crust were consistent with the velocities of granulite facies rocks found from high-pressure laboratory measurements (Christensen and Mooney, 1995; Kitamura et al., 2001). The considerable crustal evolution models to explain the velocity variations within the crust might be related to the compressional stress during the early-Paleozoic metamorphism in the Lützow-Holm Bay region (Hiroi et al., 1991; Shiraishi et al., 1994).

As for the Antarctic Peninsular, very broad Moho discontinuity was found around 36 km depths beneath PMSA (Fig. 7c, left). Several previously conducted refraction / wide-angle reflection experiments had revealed a complicated Moho topography around the region (Sroda et al., 1997; Grad et al., 2002). They determined the thickness of the crust in the range of 36-42 km at coastal area of the Peninsula, in contrast, decreased to about 25-28 km toward the Pacific Ocean. The dipping Moho obtained from our results supported a possibility of the transition zone between the oceanic and continental crust in the Antarctic Peninsula.
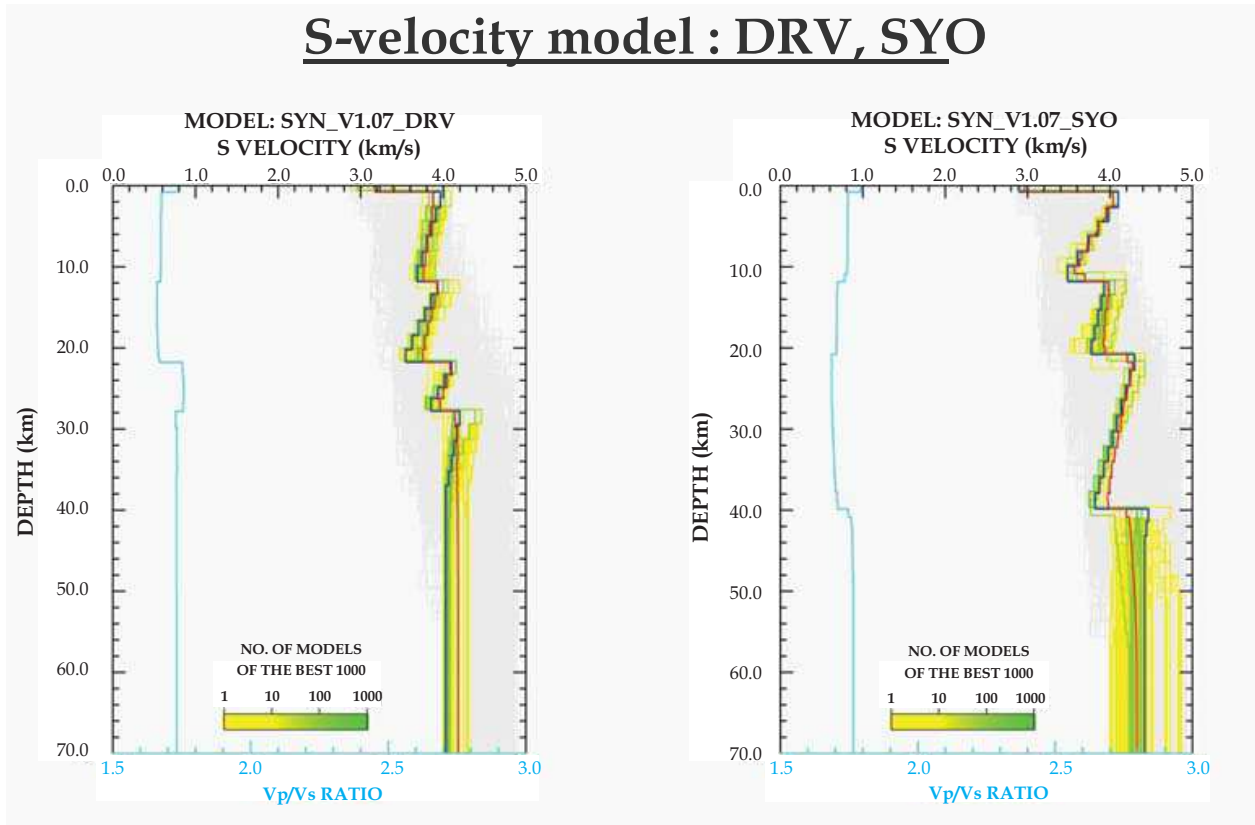
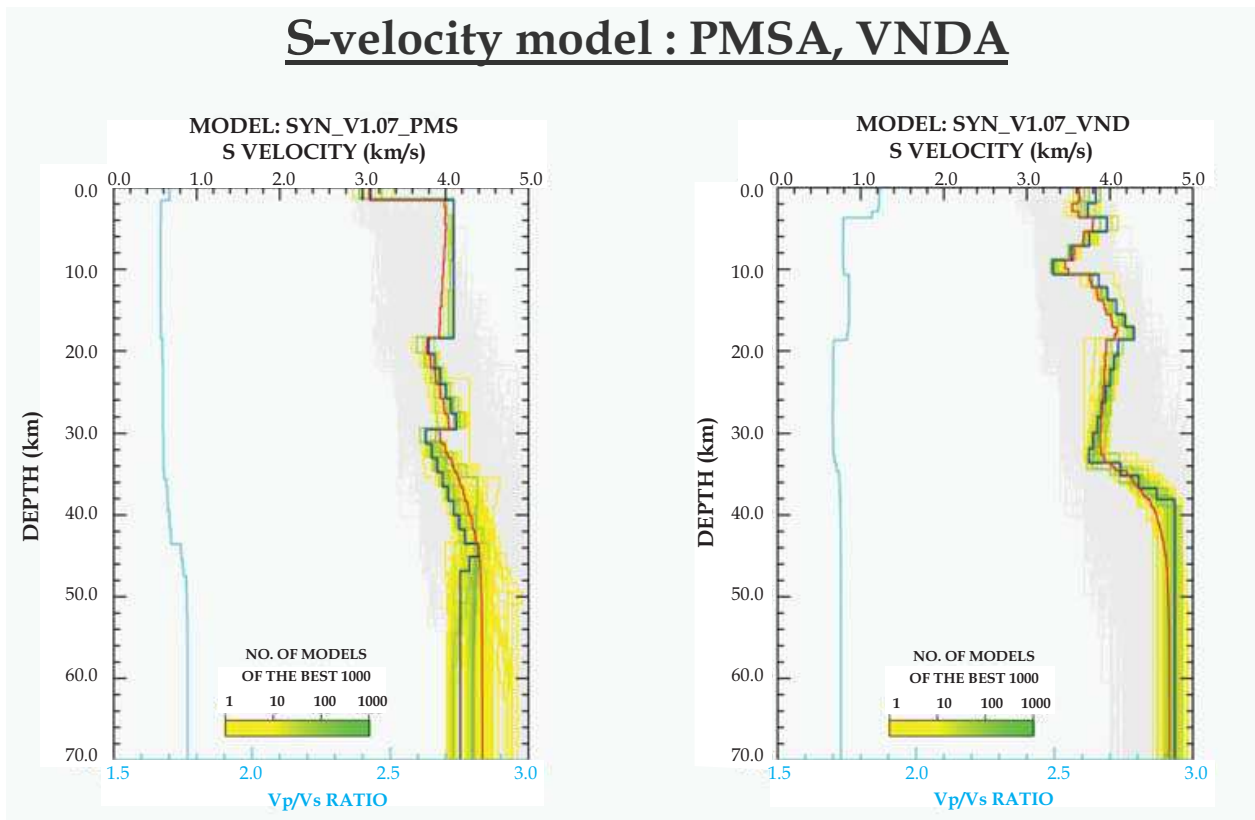Fig. 7b. Seismic S velocity models for DRV and SYO by GA inversion

Fig. 7c. Seismic S velocity models for PMSA and VNDA by GA inversion

Since the GA inversion applied for this study had assumed a uniformed structure composed of the flat-lying layers, the dipping structure cannot be directly identified. However, the obtained crust-mantle boundary was considered to reflect the averaged structure for the complicated regime in the vicinity of the Moho discontinuity.

Broadening low velocity zones around 30 km depths and transitional Moho with few km widths at VNDA (Fig. 7c, right) might be involved in the uplift mechanism on the West Antarctic Rift System (WARS) nearby the Trans Antarctic Mountains (TAM) (Smith and Drewry, 1984; Stern and ten Brink, 1989; Ten Brink et al., 1997). Around station VNDA in the Terra Nova Bay region, the Moho depth was already estimated from Ps converted phases of the receiver functions by temporary seismic array data (Di Bona et al., 1997). They pointed out a thinned crust with thickness drastically varied from 17 to 29 km, which implied a transitional zone between East and West Antarctica, which crossing the WARS. The other seismic refraction data indicated the same regime of the Moho depths involving the crustal rift system at TAM (Vedova et al., 1997). Wiens et al. (2003; 2006) conducted the TransAntarctic Mountains SEISmic experiment (TAMSEIS) around the region and obtained a detailed distribution of the crustal thickness by receiver function analyses (Lawrence et al., 2006). Their results also indicated relatively shallow Moho depths together with low velocity zones beneath VNDA.

Figure 8 demonstrated a comparison of the Moho depths by three different methods of seismic refraction studies, gravity-based estimates (after Von Frese et al., 1999), together with receiver function GA inversion by this study. In spite of the existence of small differences in estimating the Moho depths between three methods, it might be mentioned that a principal difference between the East and West Antarctica, as well as the Antarctic Peninsula, was remarkably identified. In order to establish a crustal model of the whole regions in Antarctica, available broadband waveform data of the other seismic stations, such as SPA (90.0°S), CSY (66.3°S, 110.5°E), SBA (77.8°S, 166.8°E) and the other temporary stations should be compiled for comparison.

During the International Polar Year (IPY 2007-2008), a major geo-science program had been conducted such as the 'Antarctica`s GAmburtsev Province / GAmburtsev Mountain SEISmic experiment (AGAP/GAMSEIS)' (Wiens, 2007). The AGAP/GAMSEIS was an internationally coordinated deployment with few tens of broadband seismographs over the huge area of continental ice sheet in East Antarctica. The investigations on the high plateau inside the ice covered continent could surely provide detail information on the crustal thickness and mantle structure (Hansen et al., 2010). In contrast, the 'Polar Earth Observing Network (POLENET; http://www.polenet.org/)' was another major contribution to the IPY by establishing a geophysical network mostly weighted on West Antarctica.

The accumulated seismic data during the IPY will be utilized to clarify the heterogeneous structure of the crust and upper mantle, as well as the Earth's deep interior, including the features such as the Core-Mantle-Boundary (CMB) and the lowermost mantle layer (D" zone). The broadband seismic arrays in the Antarctic at IPY and beyond have been conducting a significant contribution to FDSN as viewed from high southern latitude. Mapping of the crustal velocities beneath the whole Antarctic continent could firmly address for the advance in interpreting the difference of structure and tectonics in various terrains of Gondwana super-continent.
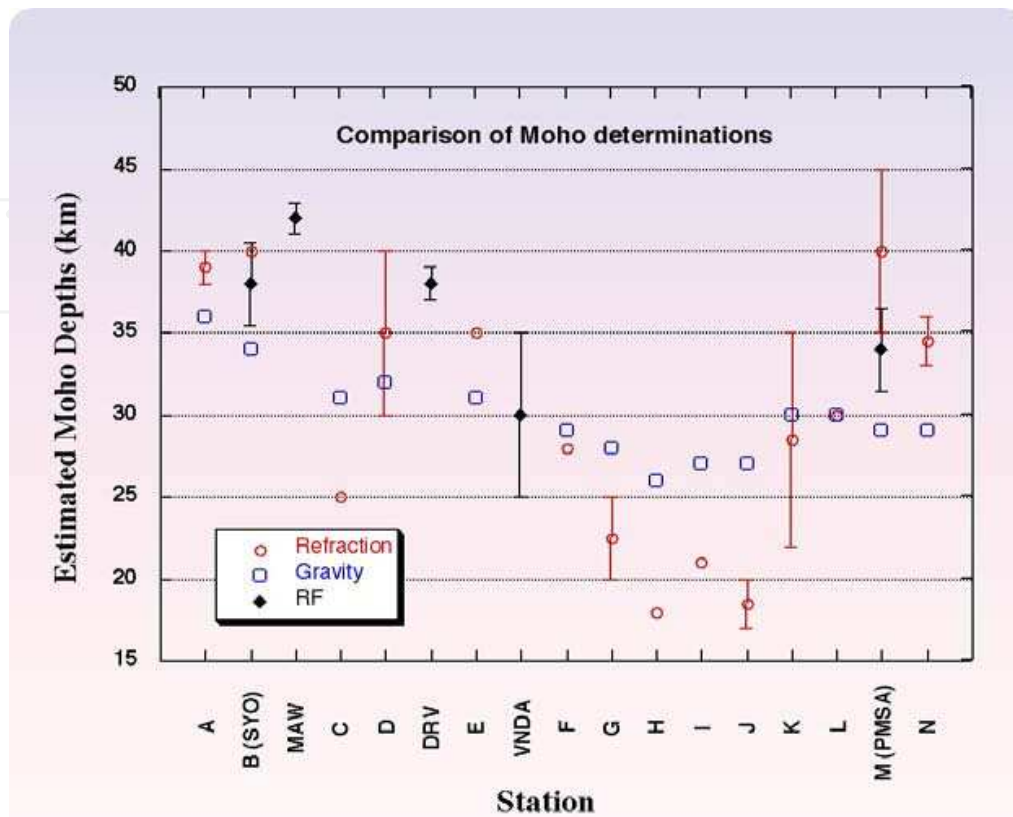
Moho depth in Antarctica

Fig. 8. Comparison of Moho depths determined from seismic refraction studies (open dots with points in center) and gravity-based estimates (open squares) (Von Frese et al., 1999), together with receiver function inversion study for permanent seismic stations (Solid diamonds; SYO, MAW, DRV, PMSA and VNDA) by this study. Alphabet numerals are location in Antarctica raveled after Von Frese et al., (1999), the same representation as in Fig. 1

4. Conclusions

In this chapter, seismic shear velocity models of the crust and the uppermost mantle were investigated by teleseismic receiver functions beneath the FDSN stations in Antarctica. In order to eliminate the starting model dependency, a non-linear GA was adopted in time domain inversion of the receiver functions. The shear velocity model beneath MAW represented a sharp Moho boundary at 44 km depth. A fairly sharp Moho was identified around 28 km and 40 km depths beneath DRV and SYO, respectively. Shear velocity variations in the crust for these stations might have a relationship with the lithologic variations of metamorphic rocks in the shallow crustal depths. Broadening low-velocity zones around 30 km depths with transitional crust-mantle boundary were identified at VNDA; which might be involved in the WARS associated with elevation of TAM. Moreover, a broad crust-mantle transition was determined around PMSA, in Antarctic Peninsula. These variations in shear velocities within the crust presumably reflected the tectonic history of each terrain where these permanent stations are belonging.

5. Acknowledgement

6. References

Ammon, C. J., Randall, G. E. & Zandt, G. (1990). On Nonuniqueness of Receiver Function Inversion, *J. Geophys. Res.*, Vol. 95, pp. 15303-15318.

Bellair, P. & Delbos, L. (1962). Age absolu de la derniere granitisation en Terre Adelie, *C. R. Ac. Sc. Paris,* Vol. 254, pp. 1465-1466.

Black, L., Harley, S. L., Sun, S. S. & McCulloch, M. T. (1987). The Rayner complex of East Antarctica: complex isotopic systematics within a Proterozoic mobile belt, *Jour. Metamor. Geol.*, Vol. 5, pp. 1-26.

Di Bona, M., Amato, A., Azzara, R., Cimini, G. B., Colombo, D. & Pondrelli, S. (1997). Constraints on the lithospheric structure benearth the Terra Nova Bay area from teleseismic P to S conversions, *In: C. A. Ricci. (ed.) The Antarctic Region: Geological Evolution and Processes, Siena, TERAPUB,* pp. 1087-1093.

Butler, R. & Anderson, K. (2008). Global Seismographic Network (GSN), *IRIS Annual Report,* pp. 6-7.

Christensen, N. I. & Mooney, W. D. (1995). Seismic velocity structure and composition of the continental crust: A global view, *J. Geophys. Res.,* Vol. 100, pp. 9761-9788.

Danesi, S. & Morelli, A. (2001). Structure of the upper mantle under the Antarctic Plate from surface wave tomography, Geophys. Res. Lett., Vol. 28, pp. 4395-4398.

Ellis, D. J. (1987). Origin and evolution of granulites in normal and thickened crusts., *Geology*, Vol. 15, pp. 167-170.

Evison, F.F., Ingham, C.E., Orr, R.H., & le Fort, J.H. (1960). Thickness of the Earth's crust in Antarctica and the surrounding oceans, *Geophys. J. R. Astron. Soc.*, Vol. 3, pp. 289-306.

Lawrence, J. F., Wiens, D. A., Nyblade. A.A., Anandakrishan, S., Shore, P. J. & Voigt, D., (2006). Upper mantle thermal variations beneath the Transantarctic Mountains inferred from teleseismic S-wave attenuation, Geophys. Res. Lett., Vol. 33, L03303, doi:10.1029/2005GL024516.

Grad, M., Guterch, A., Janik, T. & Sroda, P. (2002). Seismic characteristics of the crust in the transition zone from the Pacific Ocean to the northern Antarctic peninsula, West Antarctica, *Antarctica at the close of a millennium, Royal Society of New Zealand Bulletin*, Vol. 35, pp. 493-498.

Hansen, S. E., Nyblade, A. A., Heeszel, D. S., Wiens, D. A., Shore, P. & Kanao, M. (2010). Crustal Structure of the Gamburtsev Mountains, East Antarctica, from S-wave Receiver Functions and Rayleigh Wave Phase Velocities, *Earth Planet. Sci. Lett.*, 10.1016/j.epsl.2010.10.022.

Hiroi, Y., Shiraishi, K. & Motoyoshi, Y. (1991). Late Proterozoic paired metamorphic complexes in East Antarctica, with special reference to the tectonic significance of ultramafic rocks, *Geological Evolution of Anatrcica, M. R. A. Thomson et al. (eds.), Cambridge, Cambridge Univ. Press,* pp. 83-87.

Ikami, A. & Ito, K. (1986). Crustal structure in the Mizuho Plateau, East Antarctica, by a Two-Dimensional Ray Approximation, *Jour. Geod.*, Vol. 6, pp. 271-283.

Kanao, M. & Akamatsu, J. (1995). Shear Wave Q Structure for the Lithosphere in the Lützow-Holm Bay Region, East Antarctica,Polar Geosci., Vol. 8, pp. 1-14.

Kanao, M. (1997). Variations in the crust structure of the Lüzow-Holm Bay region, East Antarctica using shear wave velocity, *Tectonophysics,* Vol. 270, pp. 43-72.

Kanao, M., Kubo, A., Shibutani, T., Negishi, H. & Tono, Y. (2002). Crustal structure around the Antarctic margin by teleseismic receiver function analyses, *In. Antarctica at the close of a millennium, Royal Society of New Zealand Bulletin,* Vol. 35, pp. 485-491.

Kind, R., Kosarev, G. L. & Petersen, N. V. (1995). Receiver functions at the stations of the German Regional Seismic Network (GRSN), *Geophys. J. Int.*, Vol. 121, pp. 191-202.

Kitamura, K., Ishikawa, M., Arima, M. & Shiraishi, K. (2001). Laboratory measurements of P-wave velocity of granulites from Lützow-Holm Complex, East Antarctica: Preliminary report, *Polar Geosci.,* Vol. 14, pp. 180-194.

Kobayashi, R. & Zhao, D. (2004). Rayleigh-wave group velocity distribution in the Antarctic region, *Phys. Earth Planet. Inter.*, Vol. 141, pp. 167-181.

Kovach, R.L. & Press, F. (1961). Surface wave dispersion and crustal strucutre in Antarctica and the surrounding oceans, *Ann. Geofis.*, Vol. 14, pp. 211-224.

Langston, C. A. (1979). Structure under Mount Rainier, Washington, inferred from teleseismic body waves, *J. Geophys. Res.,* Vol. 84, pp. 4749-4762.

Miyamachi, H., Toda, S., Matsushima, T., Takada, M., Watanabe, A., Yamashita, M. & Kanao, M. (2003). A refraction and wide-angle reflection seismic exploration in JARE-43 on the Mizuho Plateau, East Antarctica, *Polar Geosci.,* Vol. 16, pp. 1-21.

Owens, T. J., Zandt, G. & Taylor, S. R. (1984). Seismic Evidence for an Ancient Rift Beneath the Cumberland Plateau, Tennessee: A Detailed Analysis of Broadband Teleseismic P Waveforms, *J. Geophys. Res.*, Vol. 89, pp. 7783-7795.

Ritzwoller, M. H., Shapino, N. M., Levshin, A. L. & Leahy, G. M. (2001). Crustal and upper mantle structure beneath Antarctica and surrounding oceans, *J. Geophys. Res.,* Vol. 106, pp. 30645-30670.

Roult, G., Rouland, D. & Montagner, J. P. (1994). Antarctia II: Upper-mantle structure from velocities and anisotropy, *Phys. Earth Planet. Inter.,* Vol. 84, pp. 33-57.

Sambridge, M. & Drijkoningen, G. (1992). Genetic algorithms in seismic waveform inversion, *Geophys. J. Int.,* Vol. 109, pp. 323-342.

Sheraton, J. W., Tingey, R. J., Black, L. P., Offe, L. A. & Ellis, D. J. (1987). Geology of Enderby Land and western Kemp Land, Antarctica., *Bulletin, Bureau of Mineral Resources, Australia,* Vol. 223, pp. 51.

Shibutani, T., Sambridge, M. & Kennett, B. L. (1996). Genetic algorithm inversion for receiver functions with application to crust and uppermost mantle structure beneath Eastern Australia, *Geophys. Res. Lett.,* Vol. 23, pp. 1829-1832.

Shiraishi, K., Ellis, D. J., Hiroi, Y., Fanning, C. M., Motoyoshi, Y. & Nakai, Y. (1994). Cambrian orogenic belt in East Antarctica and Sri Lanka: Implications for Gondwana assembly, J. Geology, Vol. 102, pp. 47-65.

Smith, A. G. & Drewry, D. J. (1984). Delayed phase change due to hot asthenosphere causes Transantarctic uplift ?, *Nature*, Vol. 309, pp. 536-538.

Sroda, P., Grad, M. & Guterch, A. (1997). Seismic Models of the Earth's Crustal Structure between the South Pacific and the Antarctic Peninsula, *The Antarctic Region: Geological Evolution and Processes, Siena*, pp. 685-689.

Stern, T. A. & ten Brink, U. S. (1989). Flexural uplift of the Transantarctic Mountains, *J. Goephys. Res.*, Vol. 94, pp. 10,315-10,330.

Ten Brink , U. S., Hackney, R. I., Bannister, S., Stern, T. A. & Makovsky, Y. (1997). Uplift of Transantarctic Mountains and the bedrock beneath the East Antarctic ice sheet, *J. Goephys. Res.*, Vol. 102, pp. 27,603-27,622.

Tingey, R. J. (1982). The geological evolution of the Prince Charles Mountains - an Antarctic Archaean cratonic block, *Antarctic Geoscience, C. Craddock, C. et al. (Eds.), Univ. Wisconsin Press, Madison*, pp. 455-464.

Tsuboi, S. (1995). POSEIDON (PACIFIC21), *IRIS Newsletter*, Vol. 1, pp. 8-9.

Vedova, B. D., Pellis, G., Trey, H., Zhang, J., Cooper, A. K., Marris, J. & the ACRUP Working Group (1997). Crustal structure of the Transantarcic Mountains, Western Ross Sea, *In: C. A. Ricci. (ed.) The Antarctic Region: Geological Evolution and Processes, Siena, TERAPUB,* pp. 609-618.

Von Frese, R. B., Tan, L., Kim, J. W. & Bentley, C. R. (1999). Antarctic crustal modeling from the spectral correlation of free-air gravity anomalies with the terran, *J. Geophys. Res. ,* Vol. 104, pp. 25275-25296.

Wiens D A, Anandakrishnan S, Nyblade A, Fisher J L, Pozgay S, Shore P J, Voigt D (2003): Preliminary results from the Trans-Antarctic Mountains Seismic Experiment (TAMSEIS). IX Intern. Sympo. Antarc. Earth Sci. Programme and Abstracts: 340 (September 8-12, Potsudam, Germany).

Wiens, D. A., Anandakrishnan, S. & Nyblade A. A. (2006). Remote detection and monitoring of glacial slip from Whillans Ice Streeam using seismic rayleigh waves recorded by the TAMSEIS array, *EOS Trans. AGU*, vol. 87, pp. 52.

Wiens, D. A. (2007). Broadband Seismology in Antarctica: Recent Progress and plans for the International Polar Year, *Proceedings of International Symposium –Asian Collaboration in IPY 2007-2008-*, March 1, Tokyo, Japan, pp. 21-24.

Yoshii, K., Ito, K., Miyamachi, H. & Kanao, M. (2004). Crustal structure derived from refractions and wide-angle reflections in the Mizuho Plateau, East Antarctica, *Polar Geosci.*, Vol. 17, pp. 112-138.

Young, D. N. & Ellis, D. J. (1991). The intrusive Mawson charnockites: evidence for a compressional plate margin setting of the Proterozoic mobile belt, *In. Geological Evolution of Antarctica, Thomson, M. R. A. et al. (Eds.), Cambridge, Cambridge Univ. Press,* pp. 25-31.
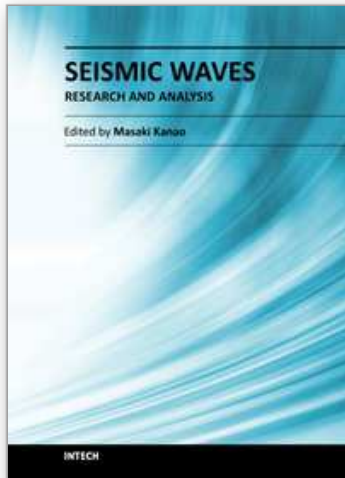
Seismic Waves - Research and Analysis

Edited by Dr. Masaki Kanao

The importance of seismic wave research lies not only in our ability to understand and predict earthquakes and tsunamis, it also reveals information on the Earth's composition and features in much the same way as it led to the discovery of Mohorovicic's discontinuity. As our theoretical understanding of the physics behind seismic waves has grown, physical and numerical modeling have greatly advanced and now augment applied seismology for better prediction and engineering practices. This has led to some novel applications such as using artificially-induced shocks for exploration of the Earth's subsurface and seismic stimulation for increasing the productivity of oil wells. This book demonstrates the latest techniques and advances in seismic wave analysis from theoretical approach, data acquisition and interpretation, to analyses and numerical simulations, as well as research applications. A review process was conducted in cooperation with sincere support by Drs. Hiroshi Takenaka, Yoshio Murai, Jun Matsushima, and Genti Toyokuni.

How to reference

In order to correctly reference this scholarly work, feel free to copy and paste the following:

Masaki Kanao and Takuo Shibutani (2012). Shear Wave Velocity Models Beneath Antarctic Margins Inverted by Genetic Algorithm for Teleseismic Receiver Functions, Seismic Waves - Research and Analysis, Dr. Masaki Kanao (Ed.), ISBN: 978-953-307-944-8, InTech, Available from: http://www.intechopen.com/books/seismic-waves-research-and-analysis/shear-wave-velocity-models-beneath-antarctic-margins-inverted-by-genetic-algorithm-for-teleseismic-r

INTECH

open science | open minds